DALTON
FULL PAPER

Synthesis of platinum(II)–piroxicam compounds. Crystal structure of *trans*-dichloro(η^2-ethene)(piroxicam)platinum(II)‡

Daniela Di Leo,[a] Francesco Berrettini[b] and Renzo Cini*,†,[a]

[a] *Department of Chemical and Biosystems Sciences and Technologies, University of Siena, Pian dei Mantellini 44, I-53100 Siena, Italy*
[b] *Interdepartmental Center for Analyses and Structural Determinations, CIADS, University of Siena, Via A. Moro, I-53100 Siena, Italy*

The reaction of Zeise's salt $K[PtCl_3(\eta^2\text{-}C_2H_4)]\cdot H_2O$ and piroxicam [4-hydroxy-2-methyl-*N*-(2-pyridyl)-2*H*-1,2-benzothiazine-3-carboxamide 1,1-dioxide, Hpir] in ethanol at room temperature produced crystalline *trans*-$[PtCl_2(\eta^2\text{-}C_2H_4)(Hpir)]\cdot 0.5C_2H_5OH$ **1**·$0.5C_2H_5OH$. Crystals of **1**·$0.5C_6H_6$ obtained from a benzene solution of **1**·$0.5C_2H_5OH$ were studied *via* X-ray diffraction techniques. The neutral piroxicam ligand co-ordinates through pyridyl N(1′) and has an *EZE* conformation typical for the neutral form. The pyridyl system of piroxicam is significantly twisted (20°) around the C(2′)–N(16) vector with respect to the rest of the ligand molecule. A comparison with previously investigated metal–piroxicam complexes shows that the C(2′)–N(16) bond is 'more flexible' than the N(16)–C(14), C(14)–C(13) and C(3)–C(4) ones. The co-ordination environment has the usual square-planar geometry for platinum(II) complexes if the middle point of the ethene C–C bond (CM) is considered. The Pt–N bond [2.093(6) Å] is longer than most Pt^{II}–N(sp^2) bond distances, because of the high *trans* influence of ethene. There is an attractive interaction between the H(N) amide atom and the Pt. The ^1H NMR spectrum of **1**·$0.5C_2H_5OH$ recorded from $CDCl_3$ solution at 22 °C shows that the signal of H(N) undergoes a shift to lower field as much as 1.98 ppm upon complexation; no ^1H–^{195}Pt coupling could be revealed. The ^1H (ethene)–^{195}Pt coupling constant is 64 Hz and spectra recorded in the temperature range −50 to 40 °C show that a fast rotation of co-ordinated ethene around the Pt–CM vector takes place at 22 °C. The reaction of potassium tetrachloroplatinate(II) with piroxicam in water at pH 8.5 gives a yellow precipitate whose formula is $Pt(pir)_2\cdot 3H_2O$, **2**·$3H_2O$. ^1H NMR data from $CDCl_3$ solutions at 22 °C are in agreement with the presence of two isomers which have been tentatively assigned to *cis*- and *trans*-$[Pt(pir)_2]$ complexes of N(1′)–O(15) chelating piroxicamate.

The high anticancer activity of cisplatin, *cis*-$[PtCl_2(NH_3)_2]$, as well as its very low solubility in physiological environments, limited spectrum of action, toxicity towards kidneys and the development of resistance by tumor cells have stimulated several research groups to synthesize and characterize new complexes of platinum and other platinum group metals.[1–4] Recently, complexes of Pt^{II} and Pt^{IV} containing a *trans*-PtX_2 function, where X is an easily removable ligand, have shown cytostatic and anticancer activities.[5,6] These observations have encouraged workers to investigate complex molecules containing the *trans*-PtX_2 group. Furthermore, the synthesis of metal complexes of pharmaceutical compounds is in general a field to be developed because the synergistic action of the beneficial effects from the ligand and the activity of the metal can provide enhanced activity of the drugs.[1–4,7]

To prepare new platinum(II) complexes with active ligands and to continue the investigation of the co-ordination chemistry of piroxicam (Scheme 1), a widely used anti-inflammatory drug, we have undertaken the synthesis and structural characterization in the solid state and in the solution phase of platinum(II)–piroxicam complexes from Zeise's salt or tetrachloroplatinate(II). The reactions of $Na_2[PdCl_4]$ with piroxicam and of Ziese's salt with 4-methylpyrimidine have also been investigated.

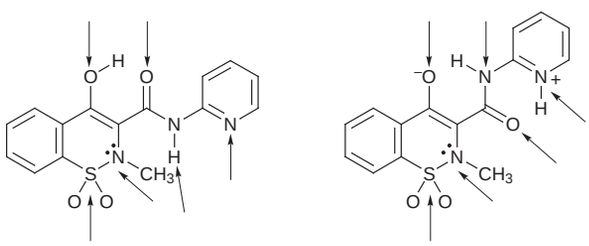

Scheme 1 Structures of two stable conformations of piroxicam. The arrows indicate possible donor sites. The protonated functions usually undergo deprotonation upon co-ordination

Experimental

Materials

Potassium tetrachloroplatinate(II), $K[PtCl_3(\eta^2\text{-}C_2H_4)]\cdot H_2O$ (both Janssen), $Na_2[PdCl_4]$ (Aldrich), 4-hydroxy-2-methyl-*N*-(2-pyridyl)-2*H*-1,2-benzothiazine-3-carboxamide 1,1-dioxide (piroxicam, Pfizer Italiana S.p.A) and 4-methylpyrimidine (mpym) (Acros) were used without further purification. The solvents dimethyl sulfoxide (dmso, analytical grade, a.g.; BDH), ethanol 99% (a.g.), diethyl ether (a.g.), methanol (a.g.) (all Baker), benzene (a.g.), chloroform (a.g.) (Merck) and chlorobenzene (a.g., Erba) were also used without any purification.

Syntheses

***trans*-Dichloro(η^2-ethene)(piroxicam)platinum(II)–ethanol (1/0.5), *trans*-$[PtCl_2(\eta^2\text{-}C_2H_4)(Hpir)]\cdot 0.5C_2H_5OH$, 1·$0.5C_2H_5OH$.** The complex $K[PtCl_3(\eta^2\text{-}C_2H_4)]\cdot H_2O$ (0.120 g, 0.3 mmol) was

† E-Mail: cini@unisi.it

‡ *Supplementary data available*: molecular mechanics parameters, IR, NMR and crystal packing diagrams. For direct electronic access see http://www.rsc.org/suppdata/dt/1998/1993/, otherwise available from BLDSC (No. SUP 57375, 16 pp.) or the RSC Library. See Instructions for Authors, 1998, Issue 1 (http://www.rsc.org/dalton).

Non-SI units employed: eV ≈ 1.60×10^{-19} J, cal = 4.184 J.

mixed with ethanol (30 cm^3) at room temperature, then filtered. A clear solution of piroxicam (0.100 g, 0.3 mmol) in ethanol (30 cm^3) was added. A pale yellow crystalline precipitate formed after a few minutes. The mixture was stirred at room temperature for 8 h and then filtered. The solid collected was rinsed with small amounts of EtOH and Et_2O, then dried and stored under vacuum. Yield 55% (Found: C, 33.67; H, 2.98; Cl, 11.13; N, 6.54; S, 4.95. Calc. for $C_{18}H_{20}Cl_2N_3O_{4.5}PtS$: C, 33.34; H, 3.11; Cl, 10.94; N, 6.48; S, 4.94%). Single crystals of **1**·0.5C_6H_6, suitable for X-ray analysis, were grown by slowly evaporating, at room temperature, a clear solution of **1**·0.5C_2H_5OH and benzene obtained by stirring the microcrystalline solid and the solvent at 50 °C.

Bis(piroxicamato)platinum(II)–water (1/3), [Pt(pir)$_2$]·3H_2O 2·3H_2O. The salt $K_2[PtCl_4]$ (0.104 g, 0.25 mmol) was dissolved in water (2 cm^3). Piroxicam (0.166 g, 0.50 mmol) was mixed with water (6 cm^3); 0.1 mol dm^{-3} NaOH was added dropwise until the pH was about 8.5 and most of the piroxicam had dissolved. The yellow solution was filtered and slowly added to the solution of the platinate(II). The pH was monitored during the addition and kept to 8.5 by adding 0.1 mol dm^{-3} NaOH. When mixing was complete the solution was stirred at 80 °C for 15 min. A pale yellow solid formed while still hot; the suspension was then stored at room temperature for 4 h. The solid was collected, washed with small amounts of EtOH and Et_2O and stored under vacuum at room temperature. Yield 45% (Found: C, 38.64; H, 2.89; N, 8.95; S, 6.85. Calc. for $C_{30}H_{30}N_6O_{11}PtS_2$: C, 39.60; H, 3.32; N, 9.24; S, 7.05%). The reaction was also carried out at 5 instead of 80 °C. After storage of the reaction mixture in a refrigerator for 3 d a yellow powder was collected, washed with EtOH and Et_2O and stored under vacuum at room temperature. Yield 30%. The infrared spectrum of this powder was superimposable on that of the precipitate obtained at 80 °C.

***trans*-Dichlorobis(piroxicam)palladium(II)–dimethyl sulfoxide (1/0.5), *trans*-[PdCl$_2$(Hpir)$_2$]·0.5dmso, 3·dmso.** The salt $Na_2[PdCl_4]$ (0.147 g, 0.5 mmol) was dissolved in dmso (5 cm^3). The orange solution was stirred at room temperature for 30 min and then filtered. Piroxicam (0.165 g, 0.5 mmol) was dissolved in dmso (5 cm^3) by stirring at 50 °C for 15 min, then added to the tetrachloropalladate(II) solution and the resulting mixture stirred at 120 °C for 20 min. The final pale yellow solution was stored at room temperature overnight. A pale yellow precipitate formed; it was collected, washed with small portions of dmso, MeOH and Et_2O and then dried in air and under vacuum at room temperature. Yield 30% (Found: C, 43.13; H, 3.41; Cl, 8.57; N, 9.86; S, 9.03. Calc. for $C_{31}H_{29}Cl_2N_6O_{8.5}PdS_{2.5}$: C, 42.35; H, 3.32; Cl, 8.06; N, 9.56; S, 9.11%). The compound is slightly soluble in dmso; it is almost insoluble in all the common solvents tested at least up to the boiling point.

***cis*-Dichlorobis(4-methylpyrimidine)platinum(II)–chloroform (1/0.5), *cis*-[PtCl$_2$(mpym)$_2$]·0.5$CHCl_3$ 4·0.5$CHCl_3$.** The compound mpym (0.055 g, 0.6 mmol) was mixed with absolute ethanol (2 cm^3), then added to a solution of K[$PtCl_3$(η^2-C_2H_4)]·H_2O (0.206 g, 0.6 mmol) in EtOH (45 cm^3). The mixture was filtered, refluxed with stirring for 1 h and then stored at room temperature for 4 h. The pale yellow precipitate was collected, rinsed with chloroform on a filter and then recrystallized from chloroform. The purified solid was stored at room temperature. Yield 35% (Found: C, 24.53; H, 2.44; N, 11.17. Calc. for $C_{10.5}H_{12.5}Cl_{3.5}N_4Pt$: C, 24.54; H, 2.45; N, 10.90%).

Spectroscopy

Proton and ^{13}C NMR spectra were recorded on a Brüker AC-200 spectrometer at 200 MHz, infrared spectra using the KBr pellet technique on a Perkin-Elmer FT-IR model 1600 machine and diffuse reflectance spectra, after dilution with KBr powder, on a Perkin-Elmer M 1800 instrument.

X-Ray crystallography

Data collection. A yellow, parallelepiped crystal (0.6 × 0.4 × 0.4 mm) of complex **1**·0.5C_6H_6 was selected, mounted on a glass fiber and used for data collection on a Siemens P4 automated four-circle diffractometer. Graphite-monochromatized Mo-Kα radiation (λ = 0.710 73 Å) was employed. Preliminary diffraction analyses carried out *via* oscillation and Weissenberg techniques performed on a Difflex R-OET machine were consistent with the triclinic system and allowed an estimation of the cell constants. Accurate cell constants (see Table 1) were then determined using the automated diffractometer *via* full-matrix least-squares refinement of the values of 28 carefully centered randomly selected reflections ($10 < \theta < 40°$). The data collected at 295 K were corrected for Lorentz-polarization and absorption effects (ψ-scan technique based on three reflections). Three standard reflections were monitored periodically (97 reflections): no appreciable decay was observed.

Structure solution and refinement. The structure solution was performed by Patterson and Fourier-difference techniques. The *R*1 and *wR*2 agreement factors (see SHELXL 93[8]) converged to 0.0422 and 0.1023 for 286 refined parameters. The H(16) and H(17) hydrogen atoms, linked to the amidic nitrogen and the enolic oxygen, respectively, were located in the Fourier-difference synthesis and freely refined in subsequent least-squares cycles. The coordinates of the four ethene ligand hydrogen atoms were not found from Fourier maps and were not included in further refinement cycles. This is because it is not possible to forecast whether the ethene ligand atoms maintain coplanarity upon co-ordination. All the other hydrogen atoms were included in the refinement in calculated positions *via* the HFIX and AFIX options of SHELXL 93.[8] All the non-hydrogen atoms were refined at the anisotropic level. The thermal parameters of all the H atoms were refined isotropically. The cocrystallized solvent molecule (benzene) is located around an inversion center so that the complex molecule and only three CH groups are present in the asymmetric unit.

The scattering factors of all the atoms were those implemented in SHELXS 86[9] and SHELXL 93.[8] The analysis of the geometrical parameters was carried out by using the PARST 95 package,[10] whereas molecular graphics and pictures were obtained by XPMA and ZORTEP.[11] All the calculations were performed on an Olidata Pentium 75 MHz personal computer and a VAX 6610 computer.

CCDC reference number 186/964.

See http://www.rsc.org/suppdata/dt/1998/1993/ for crystallographic files in .cif format.

Molecular mechanics

Molecular mechanics calculations have been carried out on a Silicon Graphics Indigo 2 machine using the MacroModel 5.0 package.[12] The total strain energy was computed as $E_{Tot} = E_b + E_\theta + E_\varphi + E_{nb} + E_{hb} + E_\varepsilon$, where E_b, E_θ, E_φ, E_{nb}, E_{hb} and E_ε are the bond length deformation, valence angle deformation, torsional angle deformation, non-bonding interaction, hydrogen-bond interaction and the electrostatic contribution, respectively; E_{hb} and E_ε have been included only when specified. The algorithm and force field ('final quality') employed were those of AMBER[13] contained in MacroModel, version 5.0. Modification of the force field was necessary in order to account for the interactions between the metal center and the ligand atoms. A trial and error method, based on the experimental crystal structures, was used. The force constants were adjusted until the root mean square deviation for the all-atom rigid superimposition of the computed and experimental

Table 1 Selected crystallographic data for *trans*-[$PtCl_2(\eta^2\text{-}C_2H_4)$(Hpir)]·0.5$C_6H_6$

Formula	$C_{20}H_{20}Cl_2N_3O_4PtS$
M	664.5
Crystal system	Triclinic
Space group	$P\bar{1}$ (no. 2)
a/Å	6.9290(10)
b/Å	11.3950(10)
c/Å	14.948(2)
α/°	87.920(10)
β/°	83.920(10)
γ/°	79.570(10)
U/Å^3	1154.0(2)
Z	2
D_c/Mg m^{-3}	1.912
μ/min^{-1}	6.49
2θ Range/°	5.48–50
Reflections collected	4435
Independent reflections (R_{int})	4071 (0.0132)
Data, restraints, parameters	3533, 5, 286
$R1$, $wR2$ ($I > 2\sigma_I$)	0.0422, 0.1023
(all data)	0.0509, 0.1136

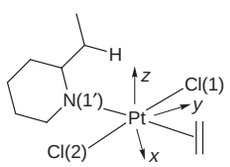

Scheme 2 Orthogonal coordinate system used for EH calculations on complex **1**

structures was less than 0.02 Å and the differences in bond distances and angles were smaller than 0.05 Å and 7.0°.

Molecular orbital calculations

The complex molecule *trans*-[$PtCl_2(\eta^2\text{-}C_2H_4)$(Hpir)] was studied by the extended-Hückel method using the CACAO PC Beta-Version 5.0 package.[14] The overlap integrals $S_{\mu\nu}$ were computed by using Slater type orbitals; the Coulomb integrals H_{ii} were considered equal to the value of the valence shell ionization energy (VSIE) of the atomic orbitals, multiplied by −1. Out of diagonal terms H_{ij} were computed *via* the formula $H_{ij} = \frac{1}{2}KS_{ij}(H_{ii} + H_{jj})$. The distance-dependent Wolfsberg–Helmholtz parameter K was used. The atomic coordinates were those obtained from the X-ray diffraction analysis. No geometry optimization was applied. The choice of the orthogonal coordinate system was as follows: z, perpendicular to the co-ordination phase, passing through Pt and pointing towards the benzothiazine moiety of Hpir; x and y, lying almost on the co-ordination plane, crossing at Pt and almost coincident with the bisectors of the Cl(2)–Pt–CM and CM–Pt–Cl(1) angles [CM = midpoint of C(1E)–C(2E) bond] (Scheme 2).

Results and Discussion

Crystal structure

The bond distances and angles are listed in Table 2. A view of the complex molecule is depicted in Fig. 1. The co-ordination geometry is square planar as usually found for platinum(II) compounds. The metal is linked to two chloride ions *trans* to each other, to the N(1′) atom from the pyridyl ring of Hpir and to an η^2-ethene molecule. The Pt–Cl distances [average 2.295(3) Å] are in perfect agreement with the values found for *trans*-[$PtCl_2$(dmso)(Hpir)] [2.295(4) Å],[15] for *trans*-[$PtCl_2$(acv)(η^2-C_2H_4)] {acv = acyclovir [9-(2-hydroxyethoxymethyl)-guanine], 2.296(1) Å},[16] for *cis*-[$PtCl(NH_3)_2$(guo-N^7)] (guo- = guanosinate) [2.295(3) Å][17] and for *cis*-[$PtCl(NH_3)_2$(tmgua)]$^+$ (tmgua = N^2,N^2,9-trimethylguanine) [2.300(2) Å].[18]

Table 2 Selected bond lengths (Å) and angles (°) for *trans*-[$PtCl_2$-(η^2-C_2H_4)(Hpir)]·0.5C_6H_6

Pt–Cl(1)	2.297(3)	O(17)–C(4)	1.334(9)
Pt–Cl(2)	2.293(3)	O(17)–H(17)	0.88(7)
Pt–N(1′)	2.093(6)	N(2)–C(3)	1.442(9)
Pt–C(1E)	2.179(11)	N(2)–C(13)	1.461(11)
Pt–C(2E)	2.148(10)	N(16)–C(14)	1.362(10)
Pt···H(16)	2.70(8)	N(16)–C(2′)	1.401(9)
C(1E)–C(2E)	1.418(14)	N(16)–H(16)	0.74(9)
S(1)–O(11)	1.430(6)	N(1′)–C(2′)	1.336(9)
S(1)–O(12)	1.421(6)	N(1′)–C(6′)	1.363(10)
S(1)–N(2)	1.639(7)	C(3)–C(4)	1.361(11)
S(1)–C(9)	1.770(8)	C(3)–C(14)	1.450(10)
O(15)–C(14)	1.239(9)	C(4)–C(10)	1.476(11)
O(15)···O(17)	2.638(8)	C(10)–C(9)	1.382(11)
N(1′)–Pt–Cl(1)	91.9(2)	O(12)–S(1)–N(2)	108.0(3)
N(1′)–Pt–Cl(2)	87.1(2)	O(12)–S(1)–C(9)	109.8(4)
Cl(1)–Pt–Cl(2)	178.8(1)	N(2)–S(1)–C(9)	101.6(3)
Cl(1)–Pt–C(1E)	88.3(3)	C(3)–N(2)–S(1)	114.0(5)
Cl(1)–Pt–C(2E)	90.1(3)	C(3)–N(2)–C(13)	113.8(6)
Cl(2)–Pt–C(1E)	92.9(3)	C(2′)–N(16)–C(14)	127.8(6)
Cl(2)–Pt–C(2E)	90.7(3)	S(1)–N(2)–C(13)	117.7(6)
N(1′)–Pt–C(1E)	159.3(3)	C(4)–C(3)–C(14)	122.0(7)
N(1′)–Pt–C(2E)	162.3(3)	H(17)–O(17)–C(4)	99(4)
N(1′)–Pt···H(16)	58(2)	C(3)–C(4)–O(17)	123.4(7)
Pt–N(1′)–C(2′)	120.0(5)	C(10)–C(4)–O(17)	114.0(7)
Pt–N(1′)–C(6′)	116.5(5)	C(3)–C(14)–O(15)	121.8(6)
Pt···H(16)–N(16)	118(4)	C(3)–C(14)–N(16)	114.9(6)
O(11)–S(1)–O(12)	119.4(4)	O(15)–C(14)–N(16)	123.3(7)
O(11)–S(1)–N(2)	107.9(3)	N(16)–C(2′)–N(1′)	114.9(6)
O(11)–S(1)–C(9)	108.5(4)	N(16)–C(2′)–C(3′)	123.6(6)

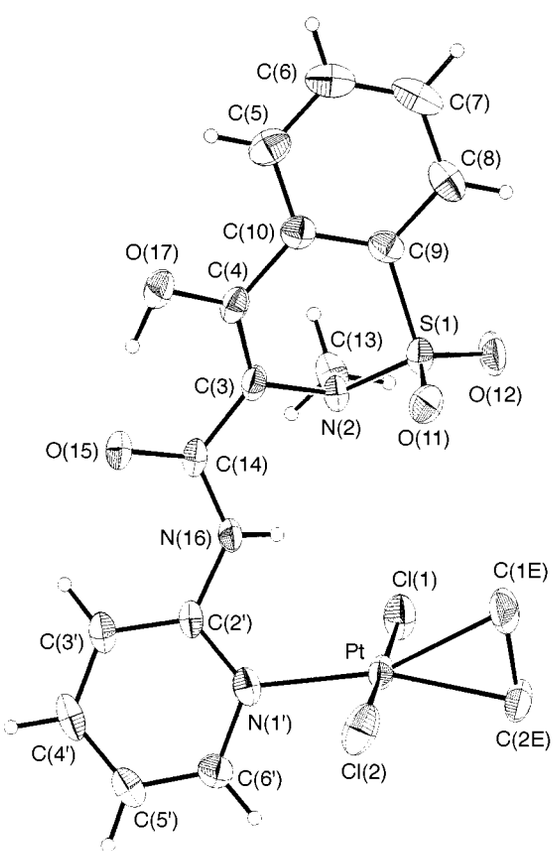

Fig. 1 A drawing of the complex molecule **1**·0.5C_6H_6 with the labeling scheme. Ellipsoids enclose 30% probability

The Pt–C(1E) and Pt–C(2E) bond distances measure 2.179(11) and 2.148(10) Å, respectively in agreement with the values previously reported for *trans*-[$PtCl_2$(acv)(η^2-C_2H_4)] [average 2.147(5) Å][16] and [$PtCl(\eta^2\text{-}C_2H_4)\{Me_2N(CH_2)_2NMe\}$]$^+$ [2.184(5), 2.166(5) Å].[19] The Pt–C distances in the anion of

Table 3 Selected Pt–N(sp^2) bond distances for square-planar platinum(II) complexes with Cl^-, I^-, NH_3, ethene and trimethylphosphine as *trans* ligand. The comparison between the listed values helps in determining the *trans* influence reported in the text

Complex	Ref.	Vector	Length/Å	R^a
cis-[$PtCl_2$(dmso)(thz)]^b	24	(Cl)–Pt–N(1)	1.989(6)	0.0425
cis-[$PtCl(NH_3)_2$(guo-N^7)]$^+$	17	(Cl)–Pt–N(7)	2.000(8)	0.0384
[$PtCl_2$(Hmbim-N^3,$N^{3'}$)]^c	25	(Cl)–Pt–N(1),N(3)	2.017(9) (average)	0.0489
cis-[$Pt(NH_3)_2$(Hguo-N^7)$_2$]$^{2+}$	26	(NH_3)–Pt–N(7),–N(17)	2.01(1) (average)	0.0420
[$Pt(NH_3)_2$(egua-N^7)$_2$]$^{2+}$	22	(NH_3)–Pt–N(7A),–N(7B)	2.024(9) (average)	0.0446
cis-[$Pt(acv)_2(NH_3)_2$]$^{2+}$	21	(NH_3)–Pt–N(7A),–N(7B)	2.02(2) (average)	0.0540
cis-[$PtCl(NH_3)_2$(tmgua)]$^+$	18	(NH_3)–Pt–N(7)	2.035(6)	0.0540
[PtI(mcyt)(egua-N^7)(NH_3)]$^{+\,d}$	27	(I)–Pt–N(7)	2.03(1)	0.0410
trans-[$PtCl_2$(dmso)(Hpir)]	15	[*S*(O)$(CH_3)_2$]–Pt–N(1′)	2.062(10)	0.0458
trans-[$PtCl_2$(acv)(η^2-C_2H_4)]	16	(η^2-C_2H_4)–Pt–N(7)	2.078(3)	0.0204
trans-[$PtCl_2$(η^2-C_2H_4)(HPir)]	Present work	(η^2-C_2H_4)–Pt–N(1′)	2.093(6)	0.0419
cis-[$Pt(Hmgua)_2(PMe_3)_2$]$^{2+\,e}$	28	(PMe_3)–Pt–N(7A),–N(7B)	2.11(1) (average)	0.0398
cis-[{Pt(mgua)$(PMe_3)_2$}$_6$]$^{6+}$	28	(PMe_3)–Pt–N(7′)	2.09(1)	0.0564
cis-[Pt(mcyt)$(PMe_3)_2$]$^{2+}$	29	(PMe_3)–Pt–N(3),–N(3′)	2.100(9) (average)	0.0670

^{a} Conventional agreement index, $R = [\Sigma||F_o| - |F_c||]/\Sigma|F_o|$. ^{b} thz = Thiazole. ^{c} Hmbim = 1-Methyl-2,2′-biimidazole. ^{d} mcyt = 1-Methylcytosine. ^{e} Hmgua = 9-Methylguanine.

Zeise's salt, [$PtCl_3$(η^2-C_2H_4)]$^-$, are slightly shorter [2.132(3) Å].[20] In agreement with the high *trans* influence of η^2-C_2H_4, the Pt–N(1′) bond distance [2.093(6) Å] is longer than the relevant values found for *cis*-[$Pt(acv)_2(NH_3)_2$]$^{2+}$ [2.02(2)],[21] *cis*-[$Pt(NH_3)_2$(egua)$_2$]$^{2+}$ (egua = 9-ethylguanine) [2.03(1) Å][22] and *cis*-[$Pt(NH_3)_2(IMP)_2$]$^{2+}$ [2.036(8) Å].[23] The Pt–N(1′) distance found in the present work is even longer than that for [$PtCl_2$(dmso)(Hpir)] [2.062(10) Å].[15]

Table 3 reports some Pt–N(sp^2) distances from the literature. From all these data the following scale of increasing *trans* influence can be arranged: $Cl^- < NH_3 \leqslant I^- < S(O)(CH_3)_2 < C_2H_4 < PR_3$. For the same ligands the *trans* effect increases in the order $NH_3 < Cl^- < I^- < S(O)(CH_3)_2 < PR_3 < C_2H_4$.[30] The metal centre deviates very slightly [0.0094(3) Å] from the plane defined by the two chloride ions, the N(1′) atom and the middle point of the C(1E)–C(2E) bond (CM), toward H(16). The deviations from the idealized values of the bond angles for the coordination plane are not significant [largest N(1′)–Pt–Cl(2) 87.1(2)°]. The largest N(sp^2)–Pt^{II}–Cl bond angles for *trans*-[$Pt^{II}Cl_2$(dmso)(Hpir)] [87.0(3)°],[15] *trans*-[$Pt^{II}Cl_2${HN=C(OH)-Bu^t}$_2$] [85.0(7)°],[30b] and {$Pt^{II}Cl_2$[HN=C(OH)Bu^t]$_2$[H_2NC(=O)-Bu^t]}$_2$ [86.7(2)°][30c] are in good agreement with the values of this work.

Ethene ligand. The ethene C–C bond is almost perpendicular to the least-squares plane defined by the donors [angle line/normal to plane 3.1(6)°] and not far from parallel to the plane of the pyridine moiety of Hpir [angle line/normal to plane 70.6(6)°]. The C–C bond distance is 1.42(1) Å, much longer than the value found for free ethene [1.337(2) Å][31] and even longer than those for *trans*-[$PtCl_2$(acv)(η^2-C_2H_4)] [1.353(8) Å][16] and for [$PtCl(\eta^2$-C_2H_4){$Me_2N(CH_2)_2NMe_2$}]$^+$ [1.376(3) Å][19] showing a large back-donation contribution for the Pt–C_2H_4 bond. The absence of any reliable model for the H atoms of ethene excludes any meaningful analysis of the deviation from planarity for η^2-C_2H_4.

Piroxicam ligand. The piroxicam ligand is in its neutral form, protonated at the phenolic oxygen [O(17)] and in the 4,16-*EZE* conformation (Scheme 1). The C(3)–(4) and C(4)–O(17) bond distances [1.36(1) and 1.334(9) Å, respectively] show significant differences when compared to the corresponding lengths for [Cd$(pir)_2(dmf)_2$] [1.396(7) and 1.276(6) Å, dmf = dimethylformamide].[32] These are explained by the different protonation status and conformation of the ligand (pir^- and *ZZZ* respectively for the latter complex).

The system C(2′)–N(16)–C(14)[O(15)]–C(3)–C(4)[O(17)]–C(10) has some degree of π conjugation on the basis of the bond lengths and coplanarity of the atoms; the H(16)–N(16)–C(14)–O(15) torsion angle measures −178°. The C(3)–C(14) length [1.450(10) Å] seems to be shorter than a C(sp^2)–C(sp^2) single bond [1.484(17) Å, 14 vectors].[33] The C(14)–N(16) vector measures 1.362(10) Å in agreement with the amide C–N bond length found for C(sp^3)–NH–C=O [1.334(11) Å, 78 vectors].[33] However, some torsion occurs around the C(2′)–N(16) bond, the N(1′)–C(2′)–N(16)–C(14) angle being 160°. This is the largest deviation from coplanarity of this portion of the molecule ever found for metal–piroxicam complexes: 11° for [$Cu(pir)_2(dmf)_2$],[32] 13° for [$PtCl_2$(dmso)(Hpir)].[15] The rotations around the N(16)–C(14), C(14)–C(3) and C(3)–C(4) bond vectors are much smaller for all the metal–piroxicam complexes (smaller than 9, 14 and 7°, respectively).

The thiazine ring has a half-chair conformation on the basis of the Cremer and Pople[34] parameters $Q_T = 0.5089(6)$ Å, $\varphi = -89.9(9)°$, $\theta = 62.4(8)°$. The S(1) and N(2) atoms deviate −0.070(2) and 0.761(6) Å, respectively, from the least-squares plane defined by the atoms C(9), C(8), C(7), C(6), C(5), C(10) and C(4). The pyridine ring atoms are strictly coplanar, the largest deviation from the least-squares plane being that of C(6′) [0.020(9) Å]. A strong intramolecular hydrogen bond between the O(17)–H group and the O(15) exists: O···O 2.638(8) Å; O–H···O 156(6)°.

The H(16) atom is 2.70(8) Å away from platinum (sum of van der Waals radii for H and Pt ranges from 2.90 to 3.25[35]) and the N(16)–H···Pt angle is 118(4)°. The H(16)···Cl(1) contact distance and the N(16)–H···Cl(1) angle are 2.72(8) Å and 144(8)°, respectively. From a comparison of the parameters reported above with those relevant to the structure of *trans*-[$PtCl_2$(dmso)(Hpir)][15] it is clear that the attractive interaction between the H(16) atom and the electron cloud located in the d_{z^2}, d_{xz} and d_{yz} orbitals of the platinum atom is weaker in the present case, in favor of a stronger intramolecular N–H···Cl hydrogen bond. The analysis of the H···Pt and H···Cl interactions is consistent with the following rationale: owing to a higher *trans* influence of ethene compared to dmso the Pt–N bond distance is longer for the ethene derivative, the H···Pt attraction is weaker, so making easier a rotation of the piroxicam molecule around the Pt–N vector (which brings the H and Cl atoms closer to each other).

The solvent molecule and the crystal packing. The cocrystallized benzene molecule has C–C bond distances ranging from 1.33 to 1.35(2) Å and almost idealized bond angles [average 120(1)°]. They do not stack with any π systems but interact with the complex molecules *via* C(1B)–H···Cl(1) hydrogen bonds [C···Cl 3.78(8) Å, C–H···Cl 143(4)°]. The complex molecules related by the inversion centre are associated *via* a network of hydrogen bonds which involve the atoms C(5) and Cl(2)

Table 4 Selected infrared absorption band maxima (cm^{-1}) for complexes **1**, **2**, **3** and free piroxicam

	1	**2**	**3**	Hpir
NH (amide)	3245.0	—	3239.3	3336.6
C=O (amide)	1656.2	1620	1655.1	1632.5
$>SO_2$	1348.9	1388.4	1346.0	1350.8

Table 5 Selected chemical shifts (ppm from tetramethylsilane) in the ^1H NMR spectra of complex **1** and free piroxicam

	δ	
	1	Hpir
H[O(17)]	12.72	13.29
H[N(16)]	10.85	8.87
H(6′)	8.59, 8.57	8.38, 8.36
H(3′)	8.45, 8.41	8.26, 8.22
H(5)	8.12–8.06	8.10–8.06
H(8)	8.00–7.91	7.95–7.90
H(4′)	8.00–7.91	7.81–7.70
H(6)	7.84–7.74	7.81–7.70
H(7)	7.84–7.74	7.81–7.70
H(5′)	7.35–7.28	7.15–7.09
H (ethene)	5.13	
H (CH_3)	3.06	2.96

[3.583(9) Å], O(17) and O(11) [3.086(8)]. Weak intermolecular stacking interactions may involve the benzo ring and the pyridyl system of piroxicam. The angle between the least-squares planes is 18.6(3)° and the contact distances between C(5) and N(1′) and C(6) and C(5′) are 3.78(1) Å. No Pt · · · Pt contact distance shorter than 4.00 Å was found.

Spectroscopy

Infrared. The wavenumbers of selected absorption maxima for compounds **1**, **2** and **3** are reported in Table 4. In the spectra of **1** and **3** the N–H stretching vibration has maxima at 3245.0 and 3239.3 cm^{-1}, respectively. It undergoes a red shift of 91.6 and 95.3 cm^{-1}, for **1** and **3**, respectively. A similar effect was found for *trans*-[$PtCl_2$(dmso)(Hpir)][15] as well as for other compounds containing the N–H function proximal to platinum atoms: *trans*-[$PtCl_2${*o*-$Ph_2PC_6H_4NHC(O)Ph_2$}$_2$],[36] *cis*-[Pt{*o*-$Ph_2PC_6H_4NC(O)C_6H_4$}{*o*-$Ph_2PC_6H_4NHC(O)Ph$}]·C_6H_5Me[37] and [Ni(CO){$NH(C_2H_4PPh_2$-2)$_3$}].[38] These data can be interpreted on the basis of a M · · · H–N interaction.

No sharp absorption band typical of the N–H amide group in the range 3500–2500 cm^{-1} can be detected in the spectrum of compound **2**. This is in agreement with a *ZZZ* conformation of the pir^- ligand in which the H–N(16) group is involved in an intramolecular hydrogen bond to O(17). The absorption band relevant to a stretching vibration for the amidic C=O group is blue-shifted for **1** and **3** (1656.2 and 1655.1 cm^{-1}) with respect to free piroxicam (1632.5), whereas it is red-shifted (1620.0) for **2** in agreement with the spectrum of [$M(pir)_2(dmf)_2$][32] in which the pir^- ligand is bidentate through N(1′) and O(15), deprotonated at O(17), and a strong N(16)–H · · · O(17) hydrogen bond exists. The band attributable to the asymmetric stretching vibration of the $>SO_2$ group is almost unchanged upon complexation for **1** and **3** whereas it is blue-shifted by some 38 cm^{-1} for **2**.

Comparison of the spectrum of complex **4** with those of the isomers *cis*- and *trans*-[$PtCl_2$(mpym)$_2$] (in the region 1000–750 cm^{-1}), reported in the literature[39] shows that the compound prepared in this work is *cis*-[$PtCl_2$(mpym)$_2$].

^1H NMR. The spectra of complex **1** and free piroxicam recorded at 22 °C from $CDCl_3$ solutions are reported in Fig. 2, chemical shifts in Table 5. All the signals are shifted towards lower field upon complexation except that for HO(17) which is

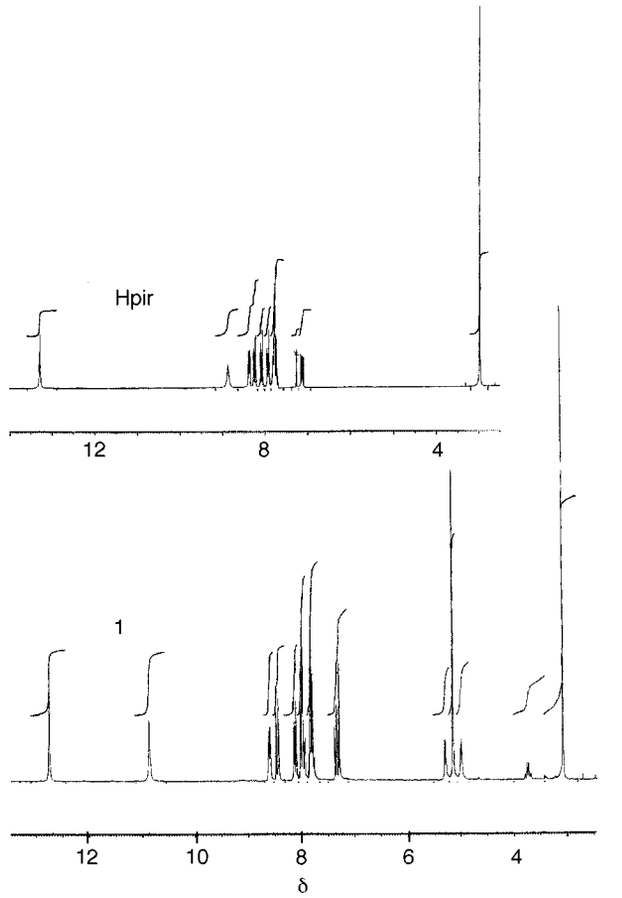

Fig. 2 Proton NMR spectra (1×10^{-2} mol dm^{-3}, $CDCl_3$, 22 °C) of free Hpir and complex **1**

upfield shifted by 0.57 ppm. The amount of the shift is usually larger for the signal of the pyridyl protons consistent with metal co-ordination to N(1′); however, the largest effect is that on the signal of H(16) (1.98 ppm). It is worth noting that no coupling between ^1H(16) and ^{195}Pt nuclei could be detected; as a consequence the Pt · · · H interaction presented above on the basis of infrared spectroscopy has no appreciable covalent component but is purely electrostatic. It is due to the partial positive charge on H and the electron clouds residing on the d orbitals with *z* character. A ^1H–^{195}Pt coupling for **1** is indeed evident from the signals around δ 5.13 [H (ethene)]: two lateral peaks are present at δ 5.29 and 4.97. The coupling constant for these nuclei is 64 Hz, larger than the values previously found for other Pt^{II}–C_2H_4 compounds which fall in the range 60–62 Hz.[16] The assignment of the peaks due to the protons of the aromatic regions reported in the literature and based on ^1H–^{13}C correlation spectra is in reasonable agreement with those for the signals of **1**.[40]

Spectra were recorded also at 40 and −50 °C for a preliminary investigation of the dynamic effects of the piroxicam and ethene moieties. The spectrum at low temperature shows extensive broadening of the peaks of the ethene protons. This is clearly attributable to a decreased rotation of ethene around the Pt–CM vector, upon cooling. On the basis of the comparison between the spectra of **1** at 40, 22 and −50 °C no rotation or conformational rearrangement for the piroxicam ligand is evident in that temperature range.

The spectrum of complex **2** shows two peaks each attributable to H–N(16) (δ 15.37, 15.87) and H_3C (δ 2.60, 2.90), respectively; their relative intensities are in a ratio of 1 : 2. It is reasonable to assume that the signals are due to two co-ordination isomers. The formation of a *cis*- and *trans*-Pt(pir)$_2$ bis(chelate), through co-ordination to N(1′) and O(15), is consistent with the infrared data (see above). The doublet centred at δ 8.97 is

attributed to H(6′) of the *trans* isomer. The spectrum of **4** (*ca.* 1×10^{-2} mol dm^{-3}) in $CDCl_3$ has peaks at δ 9.42 [1 H, H(2)], 8.89–8.87 [doublet, 1 H, H(6)], 7.22–7.20 [doublet, 1 H, H(5)] and 2.60 (3 H, methyl). Free mpym gives peaks at δ 9.03 [H(2)], 8.53–8.51 [doublet, H(6)], 7.14–7.12 [doublet, H(5)] and 2.48 (methyl).

^{13}C NMR. The chemical shifts for the signals of complex **1** (0.1 mol dm^{-3}) in $CDCl_3$ at 22 °C are reported in Table 6. It is worth noting that the signals of the pyridyl carbons are significantly shifted by 0.8–4.0 ppm towards lower fields. The signals of the benzo ring undergo small shifts of 0.2–0.6 ppm. The peaks for C(3) and C(4) move 0.3 and 1.0 ppm, those of C(2′) and C(14) 0.7 and 0.3 ppm towards higher field upon complexation. The signal of the ethene carbons is located at δ 78.7.

Molecular mechanics

The computed geometry for the structure of complex **1** is in good agreement with the experimental one in the solid state. The largest deviations are those relevant to N(1′)–C(2′) ($d_{calc} - d_{exptl}$ 0.041 Å) and to S(1)–N(2)–C(13) ($\theta_{calc} - \theta_{exptl} - 6.3°$). The root mean square deviation for the superimposition of the computed and experimental structures (all atoms) of the complex molecule is 0.091 Å. The force field parameters used in this work are reported in Table 7. The discrepancy in the N(1′)–C(2′) bond length is probably due to electronic effects induced by the N(1′)–Pt bond formation. We recall that the force field parameters for the ligand moiety used in this work are mostly those of the original AMBER.[13] The difference between computed and experimental values found for the S(1)–N(2)–C(13) bond angle must be related to intermolecular hydrogen bonds which involve the $>SO_2$ group [see above, crystal packing, O(11)].

A structure for *trans*-[$PtCl_2$(Hpir)(gua-*N*^{7})] was built starting from the computed structure of *trans*-[$PtCl_2(\eta^2$-$C_2H_4)$(Hpir)] by substituting the guanine ligand for ethene, through the graphics of MacroModel 5.0.[12] The geometry of the guanine ligand was that included in the original AMBER of MacroModel. The Pt–N(7) distance was fixed at 2.01 Å. The energy profile against rotations around the Pt–N(7) bond of such a molecule was investigated. The absolute minimum has a Cl(2)–Pt–N(7)–C(5) torsion angle of 97° (E_{tot} 152 kJ mol^{-1}) and the C(8)–H group of guanine and the $>SO_2$ group of piroxicam are *syn* to each other with respect to the coordination square. The energy profile for rotations of guanine around the Pt–N(7) vector shows two relative minima at −53 (185) and −113° (220 kJ mol^{-1}). These latter structures have the pyrimidine moiety of guanine *syn* to SO_2 of Hpir, so that O(6) and SO_2 itself have short contacts.

Table 6 Chemical shifts (ppm) in the ^{13}C NMR spectra of complex **1** and free piroxicam. See ref. 40 for assignments

	δ	
	1	Hpir
C(14)	166.5	166.9
C(4)	159.6	158.6
C(2′)	149.4	150.1
C(6′)	149.4	148.1
C(4′)	141.0	138.4
C(9)	135.2	134.6
C(6)	133.0	133.0
C(7)	133.0	132.5
C(10)	128.0	128.3
C(5)	126.9	126.7
C(8)	125.0	124.8
C(5′)	121.4	120.6
C(3′)	118.4	114.4
C(3)	111.8	111.5
C (ethene)	78.7	—
CH_3	40.6	40.0

Molecular orbital calculations

The HOMO (−11.738 eV, no. 58, Fig. 3) has relatively high percentages of p_y (7) and p_z (17%) orbitals from atom N(2) and p_x from C(3) (10) and C(4) (9%); the LUMO (−9.474 eV, no. 57) is mostly composed of p_x orbitals from C(4) (20), C(5) (16), C(7) (8), C(14) (21) and O(15) (4%). Molecular orbitals 54 (−8.265), 59 (−11.885), 60 (−11.920), 62 (−12.169) and 64 (−12.680 eV) have major components from d_{xy} (30), $d_{x^2-y^2}$ (31), d_{yz} (15), d_{xz} (41), d_{xy} (15), d_{z^2} (49), d_{yz} (22) and d_{z^2} (28); and d_{xz} (18) and d_{yz} (22%), respectively, of platinum. Molecular orbital 64 has also components of p (π) atomic orbitals from the carbon atoms of ethene and from the nitrogen atom and some carbon atoms of the pyridyl ring. This is consistent with a back donation from the metal to π* orbitals from the ligand moieties. The Mulliken analysis produced an atomic charge of 0.262 e for H(16). This (expected) positive value is consistent

Table 7 Selected force field parameters used for the molecular mechanics calculations. Other parameters are as in the original AMBER[13] included in MacroModel 5.0[12]

Vector	R_0/Å	k_r/kcal mol^{-1}	Vector	R_0/Å	k_r/kcal mol^{-1}
Pt–N(sp^2)	2.09	366	C(sp^2)–O	1.33	450
Pt–Cl	2.30	180	S=O	1.45	350
Pt–C(sp^2)	2.16	200	N(sp^3)–C(sp^3)	1.47	367
C(sp^2)–C(sp^2)	1.39	469	N(sp^3)–C(sp^2)	1.44	355
N(sp^2)=C(sp^2)	1.35	400	S–N(sp^3)	1.62	400
C(sp^2)=O	1.24	550	S–C(sp^2)	1.75	222
Angle	**θ_0/°**	**k_0/kcal rad^{-2} mol^{-1}**	**Angle**	**θ_0/°**	**k_0/kcal rad^{-2} mol^{-1}**
Cl–Pt–Cl	180	15	C(sp^2)–C(sp^2)–H	120	35
Cl–Pt–N(1′)	90	30	N(sp^2)–C(sp^2)–N(sp^2)	120	80
Cl–Pt–C	90	30	C(sp^3)–N(sp^3)–S	109	80
N(1′)–Pt–C	160	20	O=C(sp^2)–C(sp^2)	120	80
C–Pt–C	40	50	O–C(sp^2)–C(sp^2)	120	80
C–C–Pt	70	60	C(sp^2)–C(sp^2)–S	120	70
Pt–N(1′)–C(sp^2)	120	40	C(sp^2)–S–N(sp^3)	109	62
H–C(sp^2)–N(sp^2)	120	75	C(sp^2)–S=O	109	50
C(sp^2)–N(sp^2)–C(sp^2)	120	80	N(sp^3)–S=O	109	50
N(sp^2)–C(sp^2)–C(sp^2)	120	80	C(sp^3)–N(sp^3)–C(sp^2)	109	50
C(sp^2)–C(sp^2)–C(sp^2)	120	80	N(sp^3)–C(sp^2)–C(sp^2)	120	70
H–C(sp^3)–N(sp^3)	109	35	O=C(sp^2)–N(sap^2)	120	50
H–C(sp^3)–H	109	35			

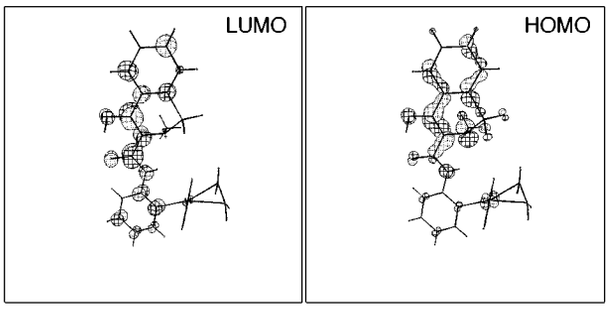

Fig. 3 Representation of the lowest unoccupied molecular orbital (LUMO) and highest occupied molecular orbital (HOMO) for complex **1**

with an attraction between the electron clouds residing in *z*-type orbitals of the metal and H(16) itself.

Conclusion

The reactivity of piroxicam with platinum(II) and palladium(II) has been tested in ethanol and water, and dmso solvents. Zeise's salt quickly reacts with piroxicam in EtOH at room temperature to produce a crystalline compound which still contains the η^2-ethene ligand. [On refluxing, the mixture of the reactants in ethanol gives a gray powder as the major product (work to investigate this material is now in progress).] The nitrogen atom from pyridyl of the piroxicam molecule has been again confirmed as the best donor site to platinum(II). As in dmso at high temperature (110 °C),[15] the ligand does not undergo deprotonation and prefers the *EZE* conformation also in an alcohol environment. The low affinity of platinum for oxygen is not able to produce deprotonation of the OH function and therefore to bring Hpir into the *ZZZ* conformation. It should be recalled that some first-row divalent 'block d' metal ions and cadmium(II) react with piroxicam in alcohol media to bring about deprotonation of the ligand and its rearrangement to the *ZZZ* conformation.[33] Deprotonation seems therefore to be a necessary preliminary step to rotations of the piroxicam molecule around the C(3)–C(14) and C(14)–N(16) vectors, to allow the *ZZZ* conformation and chelation of metals through N(1′) and O(15). Chelation *via* O(17) (deprotonated) and O(15) in an *EZE* conformation is not probable because the highly stabilizing O(17)···H–N(16) hydrogen bond would not be present. This analysis is confirmed by $[Pd^{II}Cl_2(Hpir)_2]$ **3** prepared from dmso. It contains a neutral piroxicam molecule the N–H group of which cannot interact with O(17) (protonated) and O(15) and O(17) do not interact with the metal centre. The very low solubility of **3** in all the common solvents and the failure to grow single crystals precluded complete determination of its molecular structure. However, the metal coordination to N(1′) of an *EZE* neutral piroxicam ligand is suggested by the infrared analysis. We assume a monomeric nature for the molecule, which can be *cis*- or *trans*-$[PdCl_2(Hpir)_2]$ or a mixture of the two isomers.

On mixing aqueous solutions of piroxicam and $PtCl_4^{2-}$ at pH 8.5, $[Pt(pir)_2]$ forms. Piroxicam is deprotonated under these conditions and the *ZZZ* conformation is preferred. Chelation through N(1′) and O(15) is probable, even though platinum(II) has a small affinity for oxygen atoms when compared to nitrogen (however, it has to be noted that Pt^{II}–O complexes have been previously well characterized; see for example platinum–ascorbate compounds).[41] Finally the reaction of a pyrimidine base, namely 4-methylpyrimidine, with Zeise's salt in refluxing ethanol produces *cis*-$[PtCl_2(mpym)_2]$ *via* the removal of the ethene ligand, even at a platinum : mpym molar ratio of 1 : 1.

The molecular mechanics analysis produced force field parameters suitable for simulating this class of *trans*-$[PtCl_2(\eta^2\text{-}C_2H_4)(Hpir)]$ and *trans*-$[PtCl_2(purine)(Hpir)]$ molecules. A conformational analysis of *trans*,*trans*-$[PtCl_2(Hpir)(gua\text{-}N^7)]$ in the gas phase was then performed.

Acknowledgements

R. C. thanks Consiglio Nazionale delle Ricerche (CNR, Roma) and Università degli Studi di Siena (quota 60%) for financial support. Pfizer Italiana SpA, Roma, is acknowledged for a gift of piroxicam.

References

1 M. J. Bloemink and J. Reedijk, in *Metal Ions in Biological Systems*, eds. H. Sigel and A. Sigel, M. Dekker, New York, 1996, vol. 32, pp. 641–685; J. Reedijk, *Chem. Commun.*, 1996, 801; P. M. van Vliet, *Interactions of ruthenium with purine DNA-base derivatives*, PhD Thesis, Leiden University, 1996; R. M. Roat, M. J. Jerardi, C. B. Kopay, D. C. Heath, J. A. Clark, J. A. DeMars, J. M. Weaver, E. Bezemer and J. Reedijk, *J. Chem. Soc.*, *Dalton Trans.*, 1997, 3615.
2 N. Farrell, *Transition metal complexes as drugs and chemotherapeutic agents*, Kluwer, Dordrecht, 1989; B. K. Keppler (Editor), *Metal complexes in cancer chemotherapy*, VCH, Weinheim, 1993.
3 (*a*) R. Bau, S. K. S. Huang, J.-A. Feng and C. E. McKenna, *J. Am. Chem. Soc.*, 1988, **110**, 7546; (*b*) L. J. McCaffrey, W. Henderson, B. K. Nicholson, J. E. Mackay and M. B. Dinger, *J. Chem. Soc.*, *Dalton Trans.*, 1997, 2577; (*c*) L. Bláha, I. Lukeš; J. Rohovec and P. Hermann, *J. Chem. Soc.*, *Dalton Trans.*, 1997, 2621.
4 A. Cavaglioni and R. Cini, *J. Chem. Soc.*, *Dalton Trans.*, 1997, 1149.
5 (*a*) N. Farrell, *Metal Ions in Biological Systems*, ed. H. Sigel and A. Sigel, M. Dekker, New York, 1996, vol. 32, p. 603; (*b*) G. Natile and M. Coluccia, *J. Med. Chem.*, 1993, **36**, 510.
6 L. R. Kelland, C. F. J. Barnard, K. J. Mellish, M. Jones, P. M. Goddard, M. Valenti, A. Bryant, B. A. Murrer and K. R. Harrap, *Cancer Res.*, 1994, **54**, 5618.
7 E. Ceci, R. Cini, J. Konopa, L. Maresca and G. Natile, *Inorg. Chem.*, 1996, **35**, 876.
8 G. M. Sheldrick, SHELXL 93, Program for Refinement of Crystal Structures, University of Göttingen, 1993.
9 G. M. Sheldrick, SHELXS 86, Program for Crystal Structure Determination, University of Göttingen, 1986.
10 M. Nardelli, PARST 95, A System of Computer Routines for Calculating Molecular Parameters from Results of Crystal Structures Analyses, University of Parma, 1995; *J. Comput. Chem.*, 1983, **7**, 95.
11 L. Zsolnai, ZORTEP, An interactive ORTEP program, University of Heidelberg, 1994.
12 F. Mohamadi, N. G. J. Richards, W. C. Guida, R. Liskamp, M. Lipton, C. Caufield, G. Chang, T. Hendrickson and W. C. Still, *J. Comput. Chem.*, 1990, **11**, 440.
13 S. J. Weiner, P. A. Kollman, D. A. Case, U. C. Singh, C. Ghio, G. Alagona, S. Profeta and P. Weiner, *J. Am. Chem. Soc.*, 1984, **106**, 765; S. Weiner, P. A. Kollman, D. T. Nguyen and D. A. Case, *J. Comput. Chem.*, 1986, **7**, 230; W. D. Cornel, P. Cieplak, C. I. Bayly, I. R. Gould, K. M. Merz, jun., D. M. Ferguson, D. C. Spellmeyer, T. Fox, J. W. Caldwell and P. A. Kollman, *J. Am. Chem. Soc.*, 1995, **117**, 5179.
14 C. Mealli and D. Proserpio, (*a*) CACAO PC Beta-Version 5.0, 1995; (*b*) *J. Chem. Educ.*, 1990, **67**, 399.
15 R. Cini, *J. Chem. Soc.*, *Dalton Trans.*, 1996, 111.
16 L. Cavallo, R. Cini, J. Kobe, L. G. Marzilli and G. Natile, *J. Chem. Soc.*, *Dalton Trans.*, 1991, 1867.
17 G. M. Arvanitis, D. Gibson, T. J. Emge and H. M. Berman, *Acta Crystallogr.*, *Sect. C*, 1994, **50**, 1217.
18 J. D. Orbell, C. Solorzano, L. G. Marzilli and T. J. Kistenmacher, *Inorg. Chem.*, 1982, **21**, 3806.
19 G. Gervasio, S. A. Mason, L. Maresca and G. Natile, *Inorg. Chem.*, 1986, **25**, 2207.
20 R. A. Love, T. F. Koetzle, G. J. B. Williams, L. C. Andrews and R. Bau, *Inorg. Chem.*, 1975, **14**, 2653.
21 A. Sinur and S. Grabner, *Acta Crystallogr.*, *Sect. C*, 1995, **51**, 1796.
22 B. Lippert, G. Raudaschl, C. J. L. Lock and P. Pilon, *Inorg. Chim. Acta*, 1984, **93**, 43.
23 T. J. Kistenmacher, C. C. Chiang, P. Chalilpoyil and L. G. Marzilli, *J. Am. Chem. Soc.*, 1979, **101**, 1143.
24 A. Cornia, A. C. Fabretti, M. Bonivento and L. Cattalini, *Inorg. Chim. Acta*, 1997, **255**, 405.
25 S. Karentzopoulos, H. Engelking, B. Bremer, N. Paschke and B. Krebs, *Acta Crystallogr.*, *Sect. C*, 1997, **53**, 172.
26 R. E. Cramer, P. L. Dahlstrom, M. J. T. Seu, T. Norton and M. Kashiwagi, *Inorg. Chem.*, 1980, **19**, 148.

27 T. Weinkötter, M. Sabat, G. Trötscher-Kaus and B. Lippert, *Inorg. Chim. Acta*, 1997, **255**, 361.
28 B. Longato, G. Bandoli, G. Trovò, E. Marasciulo and G. Valle, *Inorg. Chem.*, 1995, **34**, 1745.
29 G. Trovò, G. Valle and B. Longato, *J. Chem. Soc.*, *Dalton Trans.*, 1993, 669.
30 (*a*) W. L. Jolly, *The Synthesis and Characterization of Inorganic Compounds*, University of California, Berkeley, Prentice-Hall, INC., 1970; (*b*) R. Cini, F. P. Fanizzi, F. P. Intini, C. Pacifico and G. Natile, *Inorg. Chim. Acta*, 1997, **264**, 279; (*c*) R. Cini, F. P. Fanizzi, F. P. Intini, L. Maresca and G. Natile, *J. Am. Chem. Soc.*, 1993, **115**, 5123.
31 L. S. Bartell, E. A. Roth, C. D. Hollowell, K. Kuchitsu and J. E. Young, jun., *J. Chem. Phys.*, 1965, 42, 2683.
32 R. Cini, G. Giorgi, A. Cinquantini, C. Rossi and M. Sabat, *Inorg. Chem.*, 1990, **29**, 5197.
33 F. H. Allen, O. Kennard, D. G. Watson, L. Brammer, A. G. Orpen and R. Taylor, *J. Chem. Soc.*, *Perkin Trans. 2*, 1987, S1.
34 D. Cremer and J. A. Pople, *J. Am. Chem. Soc.*, 1975, **97**, 1354.
35 A. Bondi, *J. Phys. Chem.*, 1964, **68**, 441.
36 D. Hedden and D.M. Roundhill, *Inorg. Chem.*, 1985, **24**, 4152.
37 D. Hedden, D. M. Roundhill, W. C. Fultz and A. L. Rheingold, *Organometallics*, 1986, **5**, 336.
38 F. Cecconi, C. A. Ghilardi, P. Innocenti, C. Mealli, S. Midollini and A. Orlandini, *Inorg. Chem.*, 1984, **23**, 922.
39 P. C. Kong and F. D. Rochon, *Can. J. Chem.*, 1979, **57**, 526.
40 C. Rossi, A. Casini, M. P. Picchi, F. Laschi, A. Calabria and R. Marcolongo, *Biophys. Chem.*, 1987, **27**, 255.
41 L. S. Hollis, A. R. Amundsen and E. W. Stern, *J. Am. Chem. Soc.*, 1985, **107**, 274.

Received 24*th December* 1997; *Paper* 7/09280F